ISSN 1674-1056
http://cpb.iphy.ac.cn
http://iopscience.iop.org/cpb
中国物理 B
Chinese Physics
中国物理 Chinese Physics B

Role of graphene in improving catalytic behaviors of AuNPs/MoS_2/Gr/Ni-F structure in hydrogen evolution reaction

Xian-Wu Xiu(修显武), Wen-Cheng Zhang(张文程), Shu-Ting Hou(侯淑婷), Zhen Li(李振), Feng-Cai Lei(雷风采), Shi-Cai Xu(许士才), Chong-Hui Li(李崇辉), Bao-Yuan Man(满宝元), Jing Yu(郁菁), and Chao Zhang(张超)
Citation: Chin. Phys. B, 2021, 30 (**8**): 088801. DOI: 10.1088/1674-1056/abea88
Journal homepage: http://cpb.iphy.ac.cn; http://iopscience.iop.org/cpb

What follows is a list of articles you may be interested in

Enhancement of hydrogenation kinetics and thermodynamic properties of $ZrCo_{1-x}Cr_x$ (x= 0-0.1) alloys for hydrogen storage

Linling Luo(罗林龄), Xiaoqiu Ye(叶小球), Guanghui Zhang(张光辉), Huaqin Kou(寇化秦), Renjin Xiong(熊仁金), Ge Sang(桑革), Ronghai Yu(于荣海), Dongliang Zhao(赵栋梁)
Chin. Phys. B, 2020, 29 (**8**): 088801. DOI: 10.1088/1674-1056/ab9289

An overview of progress in Mg-based hydrogen storage films

Lyu Jinzhe, Andrey M Lider, Viktor N Kudiiarov
Chin. Phys. B, 2019, 28 (**9**): 098801. DOI: 10.1088/1674-1056/ab33f0

Plasma electrolytic liquefaction of sawdust

Cong-Cong Jiang(蒋匆聪), Shi-Yun Liu(刘诗筠), Zhe Feng(冯哲), Zhi Fang(方志), Xian-Hui Zhang(张先徽), Dan-Hua Mei(梅丹华), Deng-Ke Xi(席登科), Bing-Yu Luan(栾秉钰), Xing-Quan Wang(王兴权), Si-Ze Yang(杨思泽)
Chin. Phys. B, 2019, 28 (**4**): 048803. DOI: 10.1088/1674-1056/28/4/048803

420 nm thick $CH_3NH_3PbI_{3-x}Br_x$ capping layers for efficient TiO_2 nanorod array perovskite solar cells

Long Li(李龙), Cheng-Wu Shi(史成武), Xin-Lian Deng(邓新莲), Yan-Qing Wang(王艳青), Guan-Nan Xiao(肖冠南), Ling-Ling Ni(倪玲玲)
Chin. Phys. B, 2018, 27 (**1**): 018804. DOI: 10.1088/1674-1056/27/1/018804

Functionalization of carbon nanotubes/graphene by polyoxometalates and their enhanced photo-electrical catalysis

Zhang Shuang-Shuang, Liu Rong-Ji, Zhang Guang-Jin, Gu Zhan-Jun
Chin. Phys. B, 2014, 23 (**8**): 088801. DOI: 10.1088/1674-1056/23/8/088801

Role of graphene in improving catalytic behaviors of AuNPs/MoS_2/Gr/Ni–F structure in hydrogen evolution reaction*

Xian-Wu Xiu(修显武)[1,†], Wen-Cheng Zhang(张文程)[1,†], Shu-Ting Hou(侯淑婷)[1], Zhen Li(李振)[1], Feng-Cai Lei(雷风采)[2], Shi-Cai Xu(许士才)[3], Chong-Hui Li(李崇辉)[1,3,4], Bao-Yuan Man(满宝元)[1], Jing Yu(郁菁)[1,‡], and Chao Zhang(张超)[1,§]

[1] *School of Physics and Electronics, Collaborative Innovation Center of Light Manipulations and Applications, Institute of Materials and Clean Energy, Shandong Normal University, Jinan* 250014, *China*

[2] *College of Chemistry, Chemical Engineering and Materials Science, Institute of Biomedical Sciences, Shandong Normal University, Jinan* 250014, *China*

[3] *Shandong Key Laboratory of Biophysics, Institute of Biophysics, Dezhou University, Dezhou* 253023, *China*

[4] *Institute for Integrative Nanosciences, IFW Dresden, Dresden*, 01069, *Germany*

(Received 30 November 2020; revised manuscript received 5 February 2021; accepted manuscript online 1 March 2021)

The efficient production of hydrogen through electrocatalytic decomposition of water has broad prospects in modern energy equipment. However, the catalytic efficiency and durability of hydrogen evolution catalyst are still very deficient, which need to be further explored. Here in this work, we prove that introducing a graphene layer (Gr) between the molybdenum disulfide and nickel foam (Ni–F) substrate can greatly improve the catalytic performance of the hybrid. Owing to the excitation of local surface plasmon resonance (LSPR) of gold nanoparticles (NPs), the electrocatalytic hydrogen releasing activity of the MoS_2/Gr/Ni–F heterostructure is greatly improved. This results in a significant increase in the current density of AuNPs/MoS_2/Gr/Ni–F composite material under light irradiation and in the dark at 0.2 V (*versus* reversible hydrogen electrode (RHE)), which is much better than in MoS_2/Gr/Ni–F composite materials. The enhancement of hydrogen release can be attributed to the injection of hot electrons into MoS_2/Gr/Ni–F by AuNPs, which will improve the electron density of MoS_2/Gr/Ni–F, promote the reduction of H_2O, and further reduce the activation energy of the electrocatalyst hydrogen evolution reaction (HER). We also prove that the introduction of graphene can improve its stability in acidic catalytic environments. This work provides a new way of designing efficient water splitting system.

Keywords: hydrogen evolution reaction, catalytic, graphene, plasmon resonance

PACS: 88.30.em, 81.16.Hc, 61.48.Gh, 73.20.Mf **DOI:** 10.1088/1674-1056/abea88

1. Introduction

In recent years, due to the imminent global energy crisis and the serious pollution caused by fossil fuel consumption,[1] the conversion of solar energy into clean chemical fuels (H_2, CH_4, *etc.*) have been studied intensively.[2] Hydrogen is considered to be the next generation of clean and renewable energy due to its high energy density and environmentally friendly combustion products.[3,4] Hydrogen production by electrochemical splitting of water is one of the most effective and sustainable hydrogen production strategies. Precious metals play an important role in hydrogen evolution reaction (HER), such as Pt, Pd, and Rh, but the scarcity and high cost of precious metals limit its practical application.[5–7] Compared with the precious metals, non-noble metal catalysts, including enzymes, metal alloys, transition metal inorganic compounds, and metal-organic complexes, have received extensive attention and developed by various alternative methods.[8–12]

Theoretical and experimental studies have shown that materials based on two-dimensional layered molybdenum disulfide (MoS_2) will be a promising HER catalyst because the unsaturated sulfur atoms on the edges of the MoS_2 nanosheets possess excellent affinity for H_2.[13,14] Density functional theory (DFT) has demonstrated that the free energy of H adsorption on the edge of MoS_2 is neither too high nor too low ($\Delta G_H^O \cong 0$ eV).[14] As is well known, the original MoS_2 has poor electron transport performance and requires a very large overpotential to achieve a considerable HER conversion frequency. Hence, there remains a major challenge to reduce the overpotential of HER on MoS_2-based materials. In order to solve this problem, a large number of strategies have been proposed to improve the catalytic activity of MoS_2: increasing the number of active sites, enhancing the intrinsic activity, and increasing the electron transport rate.[15–17] Although great

*Project supported by the National Natural Science Foundation of China (Grant Nos. 11804200, 11974222, 11904214, and 11774208), the Project of Shandong Province Higher Educational Science and Technology Program (Grant No. J18KZ011), the Taishan Scholars Program of Shandong Province (Grant No. tsqn201812104), the Qingchuang Science and Technology Plan of the Shandong Province, China (Grant Nos. 2019KJJ014 and 2019KJJ017), China Postdoctoral Science Foundation (Grant No. 2019M662423), and the Natural Science Foundation of Shandong Province, China (Grant No. ZR201910280104).

†These authors contributed equally to this work.

‡Corresponding author. E-mail: yujing1608@sdnu.edu.cn

§Corresponding author. E-mail: czsdnu@126.com

© 2021 Chinese Physical Society and IOP Publishing Ltd

progress has been made, the current researches mainly focus on independent electrocatalysis, while neglecting the integration of other driving forces, such as photochemistry, especially the integration of local surface plasmon resonance (LSPR) to the electrocatalytic system.

The LSPR is the collective oscillating behavior of noble metal conduction electrons driven by incident light. It can provide some unique benefits as metal nanostructures, including enhanced local electromagnetic fields, effective charge carrier separation, and thermal effects during photon dissipation.[18–21] Recently, it has been demonstrated that the LSPR effect can accelerate the electrochemical process by injecting hot electrons into the catalyst.[22–26] When plasmonic metal nanostructures (such as Au, Ag, and Cu) are coupled to other substrates, such as various semiconductors (*i.e.*, TiO_2, CdS, WO_3, graphene, MoS_2, Fe_2O_3), the hot electrons excited by plasmons can overcome the Schottky barrier and be injected from metal nanoparticles into the conduction band of the semiconductor.[26–30] In addition, although AuNPs are doped into MoS_2, the doping of Au will not seriously change the crystallinity of MoS_2 nor reduce the electrical properties of the structure.[31] Therefore, the introduction of plasmonic effect into the MoS_2-based electrochemical catalyst may be an effective method to promote the entire catalytic process.

On the other hand, low-cost and well-conducted Ni foam (Ni–F) with abundant macropores has been widely used as a frame for self-supporting electrodes.[32–34] A lot of researches have been conducted on the water splitting of Ni–F framework in alkaline solution by the virtue of the well stability and at the expense of the catalytic efficiency. [34–37] Compared with that in the alkaline solution, Ni–F in the acidic solution is susceptible to chemical corrosion and unstable.[38] It has been proposed to deposit a graphene layer on Ni–F to provide strong chemical corrosion protection for long-term efficient electrocatalytic HER. Owing to its superior conductivity as an intermediate layer, graphene can effectively transfer plasmonic hot electrons quickly to form free radicals.[39] This can ensure not only the stability of the material, but also the excellent electrical conductivity of the material. In addition, Tsai *et al.* reported that the graphene layer can also adjust the hydrogen bond of the loaded MoS_2 to being closer to thermal neutrality through DFT calculations.[40]

Inspired by this, here in this work, we inject the graphene layer and Au nanoparticles that can excite the plasmonic effect into the MoS_2-based catalytic material to form the AuNPs/MoS_2/Gr/Ni–F hydrogen evolution reaction catalytic structure with strong durability and high hydrogen production efficiency. The proposed LSPR-driven AuNPs/MoS_2/Gr/Ni–F structure possesses many virtues: (i) AuNPs as light absorbers can excite electron-hole pairs in the LSPR process; (ii) MoS_2 nanosheets can act as active sites and electron acceptors to promote HER; (iii) graphene can improve the corrosion resistance of the overall structure and make the hybrid more stable. By the combination of these virtues, the hydrogen production efficiency can be enhanced by the AuNPs and MoS_2 nanosheets, and the stability can be improved by protecting the graphene. The experimental results demonstrate our expectations, *i.e.*, the excellent HER performance of the AuNPs/MoS_2/Gr/Ni–F structure with a current density of ~ 280 mA·cm^{-2} and an over potential of 28 mV are achieved when the input potential is fixed to be 0.25 V. After testing potential–current cycle (CV) characteristics1000 times, we also find that the catalytic stability is enhanced, which can be attributed to the protective effect of graphene. Our work is helpful in seeking for a versatile solution to the low efficiency and poor durability of hydrogen evolution catalyst, and paving a facile way for the popularization of hydrogen energy in the future.

2. Experiment

2.1. Structure preparation

The preparation process of AuNPs/MoS_2/Gr/Ni–F catalytic structure is shown in Fig. 1.

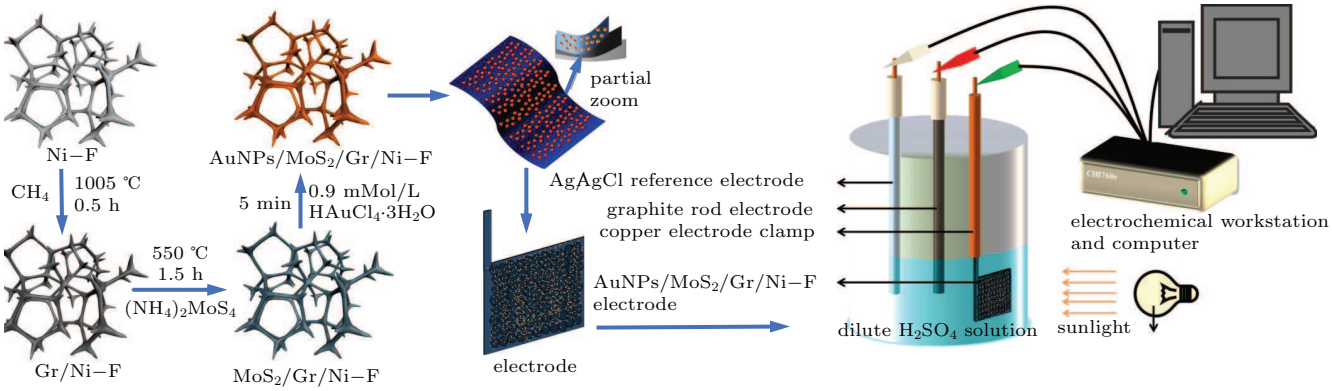


Fig. 1. Preparation process of AuNPs/MoS_2/Gr/Ni–F catalytic structure and schematic diagram for electrochemical test.

The graphene was prepared by the chemical vapor deposition (CVD) method. First, the nickel foam was cut into 1 cm×1 cm in area and cleaned with acetone, ethanol and deionized water for 1 h, in sequence. Then, the nickel foam was placed in a tubular furnace and kept for 30 min under the following condition: temperature of 1005 °C, methane flow rate of 50 sccm, and hydrogen flow rate of 50 sccm.[41,42] Then, the MoS_2 layer was prepared by thermal decomposition method and coated on the Gr/Ni–F, forming a MoS_2/Gr/Ni–F structure.[43] Finally, the MoS_2/Gr/Ni–F structure was immersed in $HAuCl_4{\cdot}3H_2O$ solution with a concentration of 0.9 mMol·L^{-1}, which was removed after 5 min. The surface residue was washed with deionized water and dried naturally, then AuNPs/MoS_2/Gr/Ni–F catalytic structure with an area of 1 cm^2 was prepared.

2.2. Characterization of samples

The Raman spectra were recorded with a Raman spectrometer (Horiba Lab RAM HR Evolution 800). The wavelength and power of laser were 532 nm and 0.48 mW, respectively with a diffraction grid of 600 g·nm^{-1}. A 50× objective was used to focus the laser beam on the substrate. The scanning electron microscope (SEM) and energy dispersive spectroscopy (EDS) test were carried out using a scanning electron microscope (ZEISS Sigma500 at 5.0 kV).

2.3. Electrochemical detection

Using a three-electrode system, AuNPs/MoS_2/Gr/Ni–F sample with a size of 1 cm×1 cm was used as a working electrode and clamped by copper electrode, the graphite rod was used as a counter electrode, and the Ag/AgCl electrode was used as a reference electrode. Using solar simulator as the light condition, a series of electrochemical tests was carried out on the three-electrode system in a H_2SO_4 environment with a concentration of 0.5 mol·L^{-1}.

3. Results and discussion

The scanning electron microscope SEM images are carried out to characterize the morphologies of the samples as shown in Figs. 2(a)–2(d). As shown in Fig. 2(a), before the deposition of the graphene, the surface of the Ni–F material is smooth and flat. After the growth of the graphene as shown in Fig. 2(b), the surface of Gr/Ni–F structure turns black and wrinkled morphology, which demonstrates that the graphene layer is highly uniformly covered on the Ni–F. The image of Raman spectrum in the insert of Fig. 2(b) exhibits two characteristic peaks of graphene at −1580 cm^{-1} (G band) and −2700 cm^{-1} (2D band), which further proves the existence of graphene. After the growing of MoS_2 by thermal decomposition in Fig. 2(c), it can be seen clearly that MoS_2 film on the surface of MoS_2/Gr/Ni–F structure is fragmented, which can increase the effective reaction area and the number of active sites for the hydrogen evolution. The characteristic peaks (E_{2g} and A_{1g} modes, respectively) of MoS_2 at 386 cm^{-1} and 406 cm^{-1} shown in the image of Raman spectroscopy further indicate that a high-quality MoS_2 layer is deposited.[43] In order to endow the MoS_2/Gr/Ni–F with plasmonic activity, the sample was soaked in a 0.9-mMol·L^{-1} $HAuCl_4{\cdot}3H_2O$ aqueous solution for 5 min to obtain AuNPs/MoS_2/Gr/Ni–F. As exhibited in Fig. 2(d), the AuNPs are evenly distributed with moderate density and high coverage, which provides an excellent platform for the generation of plasmonic effect and builds a perfect stage for the catalytic hydrogen evolution reaction.[44] In addition, to further characterize the AuNPs/MoS_2/Gr/Ni–F structure, the EDS element mapping corresponding to the structure is shown in Fig. 2(e), which clearly shows the coexistence of Au, Mo, S, and C elements. As can be seen from the distribution of Au, S, and Mo elements in Fig. 2(e), AuNPs and MoS_2, which play a key catalytic role, are uniformly distributed. In order to confirm the plasmonic enhancement effect of AuNPs, we compare the Raman spectra of MoS_2 on the MoS_2/Gr/Ni–F sample and AuNPs/MoS_2/Gr/Ni–F sample.

Figure 2(f) presents the change of the Raman characteristic peak of MoS_2. We can see clearly that the intensity of Raman peak of MoS_2 is greatly enhanced by the addition of AuNPs, which can be attributed to the electromagnetic enhancement based on the LSPR effect introduced by the AuNPs. The LSPR of AuNPs is much beneficial for the improvement of the catalytic hydrogen evolution performance and will be discussed in detail later, which can reduce the overpotential of the MoS_2 layer in the hydrogen evolution reaction and greatly increase the electron transfer rate.[45] The x-ray photoelectron spectroscopy (XPS) spectra show that the binding energies of Au $4f_{5/2}$ and Au $4f_{7/2}$ in AuNPs/MoS_2/Gr/Ni–F are positively shifted by approximately 0.20 eV and 0.14 eV, respectively, compared with those of AuNPs/Gr/Ni–F (Fig. 2(g)). The binding energies of Mo $3d_{3/2}$ and Mo $3d_{5/2}$ in AuNPs/MoS_2/Gr/Ni–F are negatively shifted by approximately 0.21 eV and 0.23 eV respectively, as compared with those in MoS_2/Gr/Ni–F (Fig. 2(h)). The binding energies of S $2p_{3/2}$ in AuNPs/MoS_2/Gr/Ni–F are negatively shifted by approximately 0.18 eV, respectively, as compared with those in MoS_2/Gr/Ni–F (Fig. 2(i)). These results unambiguously confirm that the electrons transfer from AuNPs to MoS_2 in AuNPs/MoS_2/Gr/Ni–F.

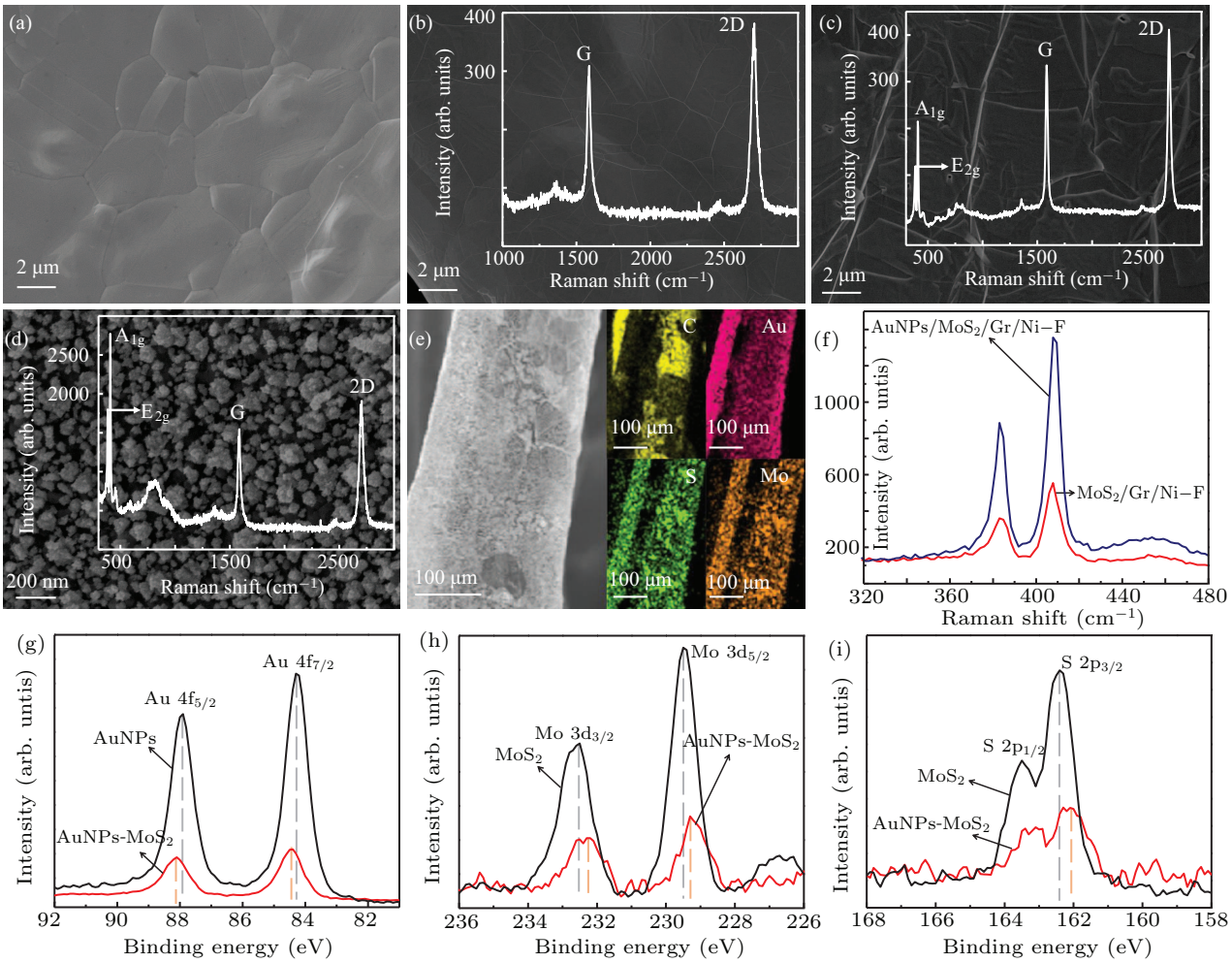


Fig. 2. (a) SEM image of Ni–F, (b) SEM image and Raman spectrum image of Gr/Ni–F, (c) SEM image and Raman spectrum image of MoS_2/Gr/Ni–F, (d) SEM image and Raman spectrum image of AuNPs/MoS_2/Gr/Ni–F, (e) EDS image of AuNPs/MoS_2/Gr/Ni–F, (f) Raman spectra of the MoS_2 on AuNPs/MoS_2/Gr/Ni–F and MoS_2/Gr/Ni–F, (g) Au 4f XPS spectra of AuNPs/MoS_2/Gr/Ni–F and AuNPs/Gr/Ni–F, (h) Mo 3d XPS spectra of AuNPs/MoS_2/Gr/Ni–F and MoS_2/Gr/Ni–F, and (i) Mo 3d XPS spectra of AuNPs/MoS_2/Gr/Ni–F and MoS_2/Gr/Ni–F.

Since the structure of metal nanoparticles will affect the plasmonic effect and further influence the plasmonic enhancement process, we investigate the optimal immersed time for the better plasmonic enhanced effect by using Raman spectrum.[46] We immerse the MoS_2/Gr/Ni–F in $HAuCl_4{\cdot}3H_2O$ with a concentration of 0.9 mMol·L^{-1} for different times, and then collect the Raman spectrum of the MoS_2. As can be seen from Fig. 3(a), the characteristic peaks of MoS_2 can be clearly observed in all samples and increase with the immersed time increasing, the intensities of Raman peaks of MoS_2 increase with the immersed time increasing from 1 min to 5 min. However, further increasing the immersed time, the intensities of the peaks will decrease. The variations of the Raman peaks' intensities with the different immersed time are further plotted and exhibited in Fig. 3(b). In order to ascertain why the Raman intensity behaves so, we collect the SEM images of the samples with different immersed times as shown in Fig. 3(c). As can be seen from Fig. 3(c), the gap between the AuNPs on the surface of the sample is larger when the immersed time is within 5 min, therefore the plasmonic effect is weak. Further increasing the immersed time, AuNPs form bigger cluster and the gap between the AuNPs is partially filled, which results in the decrease of the hot spots and the weak plasmonic effect. Hence, the optimal immersed time for the plasmonic effect is achieved to be 5 min.

To investigate the enhancement of the LSPR effect introduced by AuNPs for the catalytic hydrogen evolution performance, we measure the electrocatalytic HER activities of the AuNPs/MoS_2/Gr/Ni–F and the MoS_2/Gr/Ni–F in 0.5-mol·L^{-1} H_2SO_4 using a typical three-electrode setup at room temperature. We can see clearly that in the polarization curve (I–V diagram) shown in Fig. 4(a), under an overpotential of 0.25 V, a current density of $\sim$ 250 mA·cm^{-2} can be achieved for the case of the AuNPs/MoS_2/Gr/Ni–F under the dark, which is much larger than that ($\sim$ 55 mA·cm^{-2}) of the MoS_2/Gr/Ni–F under the same condition, indicating the enhancement effect due to charge interaction between AuNPs and MoS_2/Gr/Ni–F.[47] Under illumination, the current density of AuNPs/MoS_2/Gr/Ni–F increases from $\sim$ 250 mA·cm^{-2} to $\sim$ 280 mA·cm^{-2} (increased by 12%),

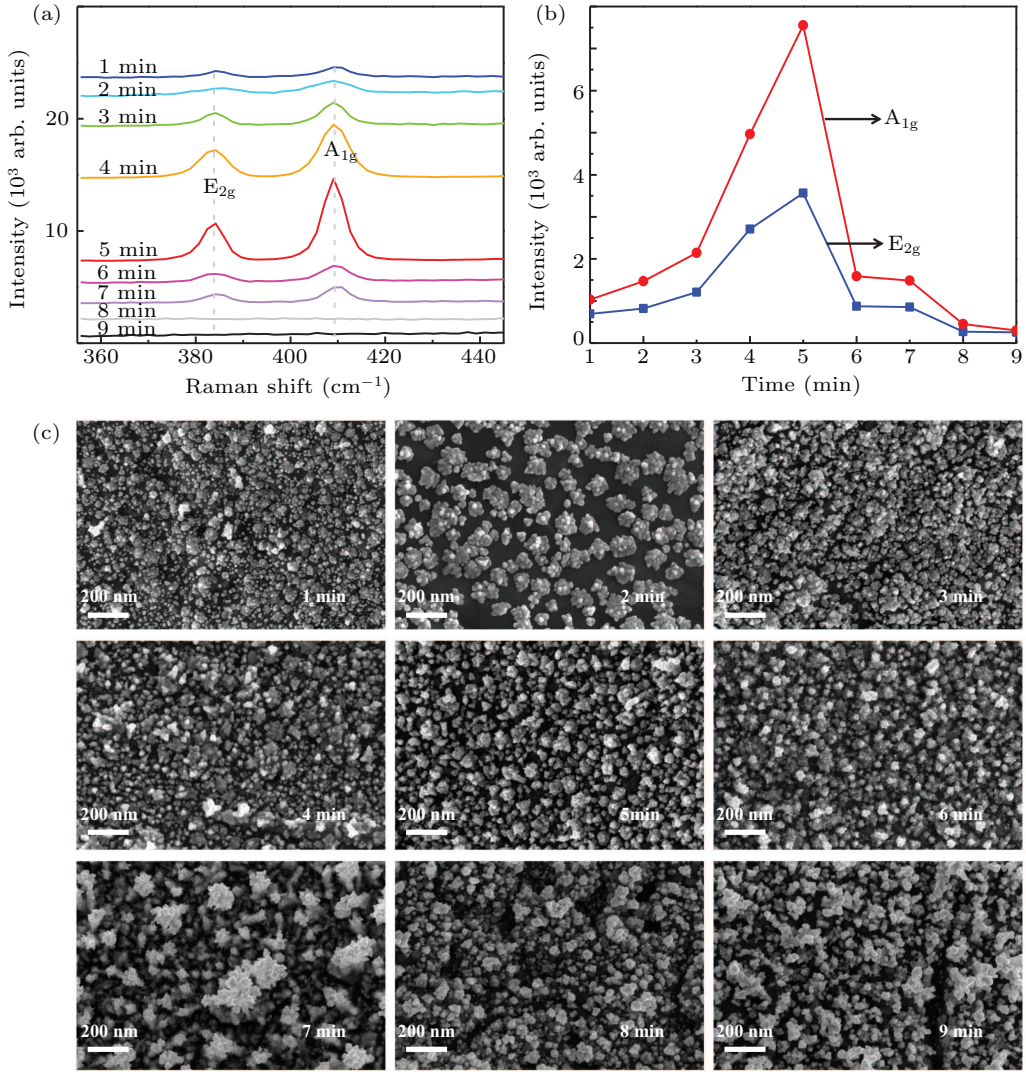


Fig. 3. (a) Raman peaks of MoS_2 after putting MoS_2/Gr/Ni–F in $HAuCl_4{\cdot}3H_2O$ varying with time, (b) intensities of two Raman characteristic peaks varying with time of MoS_2, and (c) corresponding SEM images of MoS_2/Gr/Ni–F at different times.

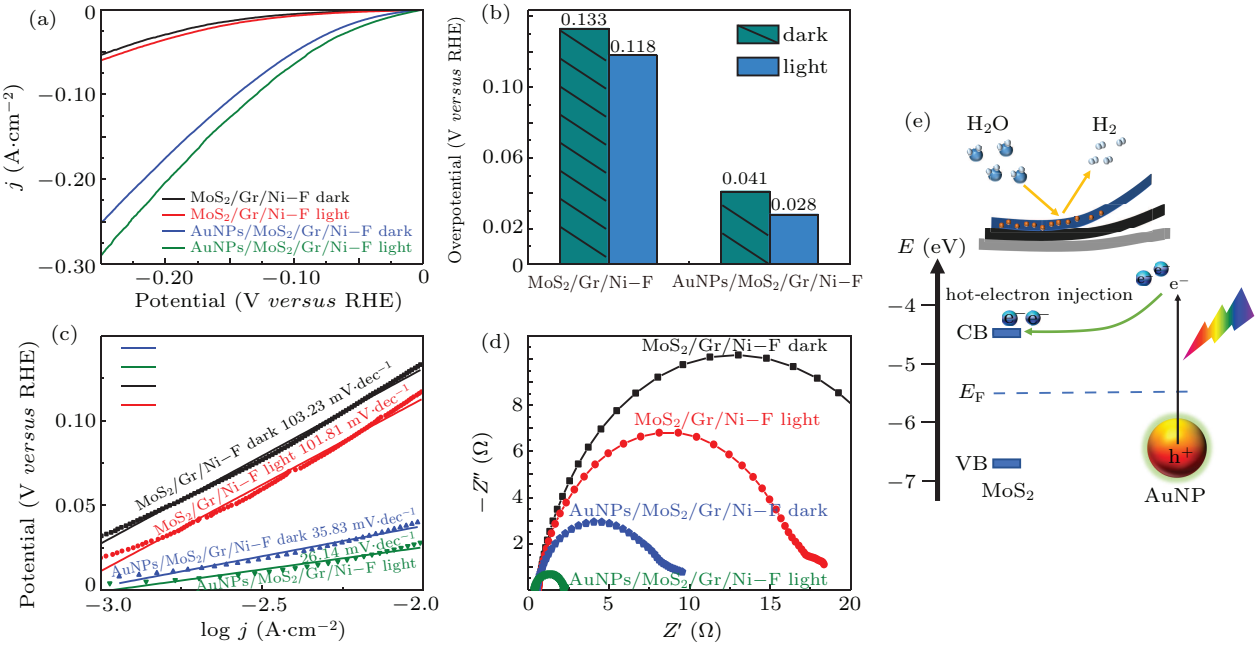


Fig. 4. (a) Linear sweep voltammetry (LSV) curve of MoS_2/Gr/Ni–F and AuNPs/MoS_2/Gr/Ni–F under dark and light, (b) overpotential of MoS_2/Gr/Ni–F and AuNPs/MoS_2/Gr/Ni–F under dark and light, (c) Tafel slope graph of the MoS_2/Gr/Ni–F and AuNPs/MoS_2/Gr/Ni–F under dark and light, (d) corresponding electrochemical impedance spectroscopy (EIS) Nyquist plots, (e) illustration of mechanism of HER with MoS_2/Gr/Ni–F.

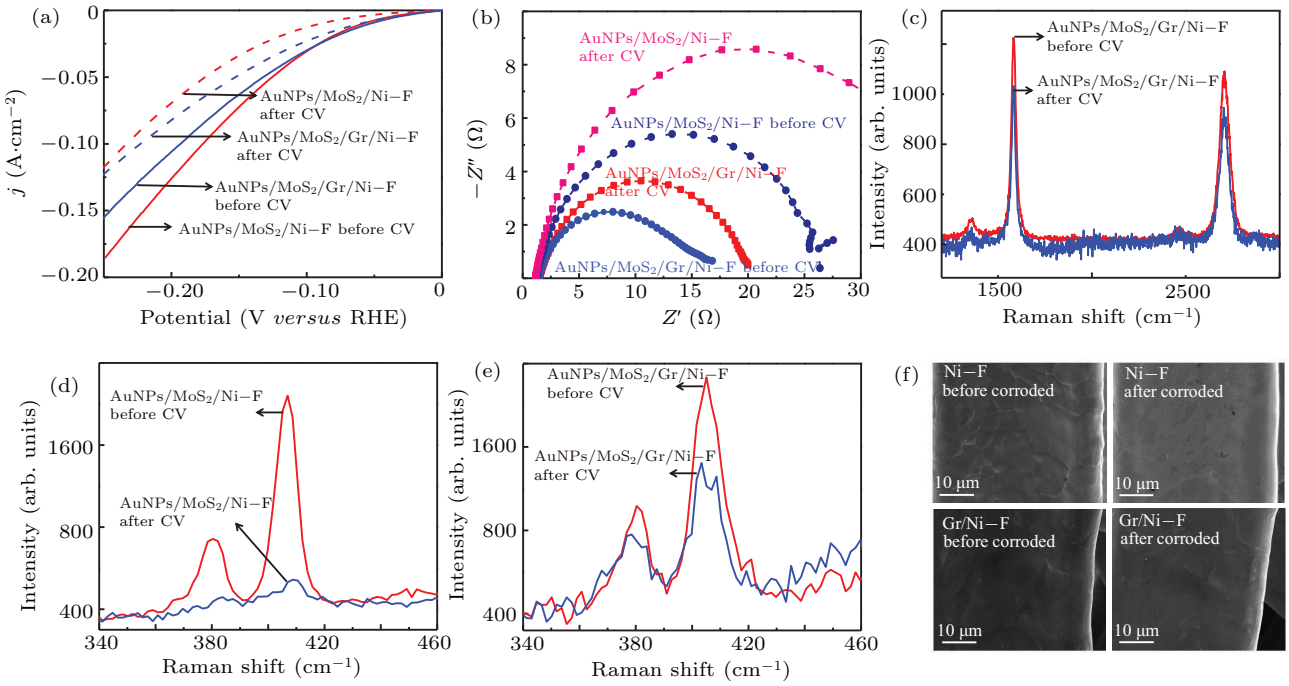


Fig. 5. (a) Comparison between LSV curves of AuNPs/MoS_2/Ni–F and AuNPs/MoS_2/Gr/Ni–F before and after 1000-CV tests, (b) EIS test Nyquist plots, (c) Raman spectra of graphene in the AuNPs/MoS_2/Gr/Ni–F before and after 1000-CV tests, (d) Raman spectra of MoS_2 in the AuNPs/MoS_2/Ni–F before and after 1000-CV tests, (e) Raman spectra of MoS_2 in the AuNPs/MoS_2/Gr/Ni–F before and after 1000-CV tests, and (f) SEM images of Ni and Gr/Ni before and after corrosion by dilute H_2SO_4.

while there is almost no improvement for the case of MoS_2/Gr/Ni–F. The slight increase in MoS_2/Gr/Ni–F data is due to the photocatalytic properties of MoS_2 itself.[48] These results show that the LSPR effect of AuNPs can increase the polarization current density of the sample electrode. Under a current density of 10 mA·cm^{-2}, AuNPs/MoS_2/Gr/Ni–F exhibits the lowest overpotential (0.028 V) in all samples (see Fig. 4(b)). The trend is similar to the result shown in Fig. 4(a). Based on the polarization curves in Fig. 4(a), the corresponding Tafel plots are further calculated to evaluate the influence of charge interaction and LSPR on the HER kinetics. The Tafel slope of AuNPs/MoS_2/Gr/Ni–F under the light (26.14 mV·dec^{-1}) is much lower than that of MoS_2/Gr/Ni–F under the dark (103.23 mV·dec^{-1}), MoS_2/Gr/Ni–F under the light (101.81 mV·dec^{-1}), and AuNPs/MoS_2/Gr/Ni–F under the dark (36.83 mV·dec^{-1}), suggesting its more favorable HER kinetics (see Fig. 4(c)).[49,50] Furthermore, figure 4(d) shows various Nyquist plots. The electrochemical impedance spectroscopic measurements are conducted at an overpotential of 300 mV in a frequency range from 10 kHz to 0.1 Hz. Obviously, the AuNPs/MoS_2/Gr/Ni–F under the light shows an extremely small diameter semicircle, indicating the minimal charge transfer resistance. This clearly indicates the accelerated HER kinetics by light-induced LSPR of AuNPs. Based on the above results, figure 4(e) shows the expected mechanism between Au and MoS_2 for enhancing HER activity. The high-energy hot electrons generated on AuNPs based on the LSPR will escape from the electronic equilibrium state. When the plasmon-induced hot electrons are injected from AuNPs into MoS_2, the excited plasmons will be relaxed. This non-radiative relaxation of LSPR will significantly improve the light absorption performance of the catalyst.[51]

As mentioned above, graphene in the AuNPs/MoS_2/Gr/Ni–F structure has strong corrosion protection, especially in an acidic environment, which allows the surface of the catalyst structure remain intact to maintain the original catalytic performance. In order to verify this effect, we test the cyclic CV characteristic cycle 1000 times to observe the durability of the sample. To demonstrate this point, a control sample (AuNPs/MoS_2/Ni–F) is prepared. The AuNPs/MoS_2/Ni–F sample and AuNPs/MoS_2/Gr/Ni–F sample are CV-tested 1000 times under acidic three-electrode system. Under an overpotential of 0.25 V, the current density of AuNPs/MoS_2/Ni–F drops from $\sim$ 184 mA·cm^{-2} to $\sim$ 117 mA·cm^{-2} (a drop of 36.4%) after having been CV-tested 1000 times, at the same time AuNPs/MoS_2/Gr/Ni–F drops from $\sim$ 155 mA·cm^{-2} to $\sim$ 122 mA·cm^{-2} (A drop of 21.2 % only) (Fig. 5(a)). We further carry out the EIS test. After being CV-tested 1000 times, the AuNPs/MoS_2/Gr/Ni–F changes much less than ton the AuNPs/MoS_2/Ni–F (Fig. 5(b)).

This shows that the existence of graphene can keep the material's original small charge transfer resistance. After being CV-tested 1000 times, we collect the Raman spectra of graphene, where only a slight decrease is observed, indicating that the graphene is stably attached to the Ni–F framework and will not fall during electrochemical tests in the electrolyte as shown in Fig. 5(c).

Figures 5(d) and 5(e) show the comparison between Raman spectra of AuNPs/MoS_2/Ni–F and AuNPs/MoS_2/Gr/Ni–

F before and after having been CV-tested 1000 times, where we can see that the Raman intensity of MoS_2 on the AuNPs/MoS_2/Gr/Ni–F has almost no change while that on the AuNPs/MoS_2/Ni–F decreases greatly. In order to further verify the stability and corrosion resistance provided by the graphene layer in the AuNPs/MoS_2/Gr/Ni–F catalytic structure, we immerse the Ni–F and Gr/Ni–F in 0.5-mol·L^{-1} H_2SO_4 for 12 h, and collect the SEM images of the surface morphology before and after corrosion. It can be seen from Fig. 5(f) that after being immersed for 12 h, the original surface protrusions of the Ni–F are corroded round and smooth. In contrast, after being immersed, the surface morphology of Gr/Ni–F is hardly changed, and the wrinkle characteristics of the two-dimensional film can still be seen. In short, we confirm that the combination of graphene and molybdenum disulfide to prepare a heterojunction can exert the excellent mechanical strength and flexibility of graphene, as a result, the stability of the hybrid can be greatly improved even in the complex environment.

4. Conclusions

In this work, our constructed AuNPs/MoS_2/Gr/Ni–F structure is a stable and efficient HER electrocatalyst with LSPR characteristics. Upon light irradiation, the overpotential at a current density of 10 mA·cm^{-2} decreases from 41 mV to 28 mV and the current density realizes an enhancement. As evidenced by photoelectrochemical analysis results, this enhanced activity relies on the efficient injection of hot electrons from plasmonic AuNPs into MoS_2/Gr/Ni–F under light irradiation. In addition, the HER activation energy decreases significantly due to the LSPR effect under light irradiation. We demonstrate that the introduction of graphene can improve the stability in an acidic catalytic environment. It is believed that these findings will provide new ways to design high-performance water electrolysis systems.

References

[1] Wang C C, Li J R, Lv X L, Zhang Y Q and Guo G 2014 *Energy Environ. Sci.* **7** 2831
[2] Chu S and Majumdar A 2012 *Nature* **488** 294
[3] Dresselhaus M S and Thomas I L 2001 *Nature* **414** 332
[4] Turner J A 2004 *Science* **305** 972
[5] Zou X and Zhang Y 2015 *Chem. Soc. Rev.* **44** 5148
[6] Roger I, Shipman M A and Symes M D 2017 *Nat. Rev. Chem.* **1** 1
[7] Li Y, Wang H, Xie L, Liang Y, Hong G and Dai H 2011 *J. Am. Chem. Soc.* **133** 7296
[8] Popczun E J, McKone J R, Read C G, Biacchi A J, Wiltrout A M, Lewis N S and Schaak R E 2013 *J. Am. Chem. Soc.* **135** 9267
[9] Kibsgaard J, Chen Z, Reinecke B N and Jaramillo T F 2012 *Nat. Mater.* **11** 963
[10] Chen W F, Sasaki K, Ma C, Frenkel A I, Marinkovic N, Muckerman J T, Zhu Y and Adzic R R 2012 *Angew. Chem.-Int. Edn.* **51** 6131
[11] Andreiadis E S, Jacques P A, Tran P D, Leyris A, Chavarot-Kerlidou M, Jousselme B, Matheron M, Pécaut J, Palacin S, Fontecave M and Artero V 2013 *Nat. Chem.* **5** 48
[12] Vrubel H and Hu X 2012 *Angew. Chem.-Int. Edn.* **51** 12703
[13] Jaramillo T F, Jørgensen K P, Bonde J, Nielsen J H, Horch S and Chorkendorff I 2007 *Science* **317** 100
[14] Hinnemann B, Moses P G, Bonde J, Jørgensen K P, Nielsen J H, Horch S, Chorkendorff I and Nørskov J K 2005 *J. Am. Chem. Soc.* **127** 5308
[15] Xie J, Zhang J, Li S, Grote F, Zhang X, Zhang H, Wang R, Lei Y, Pan B and Xie Y 2013 *J. Am. Chem. Soc.* **135** 17881
[16] Lukowski M A, Daniel A S, Meng F, Forticaux A, Li L and Jin S 2013 *J. Am. Chem. Soc.* **135** 10274
[17] Li Y, Wang H, Xie L, Liang Y, Hong G and Dai H 2011 *J. Am. Chem. Soc.* **133** 7296
[18] Zhang C, Jiang S Z, Huo Y Y, Liu A H, Xu S C, Liu X Y, Sun Z C, Xu Y Y, Li Z and Man B Y 2015 *Opt. Express* **23** 24811
[19] Xu J, Li C, Si H, Zhao X, Wang L, Jiang S, Wei D, Yu J, Xiu X and Zhang C 2018 *Opt. Express* **26** 21546
[20] Zhang C, Li C, Yu J, Jiang S, Xu S, Yang C, Liu Y J, Gao X, Liu A and Man B 2018 *Sens. Actuator B-Chem.* **258** 163
[21] Wang C, Nie X G, Shi Y, Zhou Y, Xu J J, Xia X H and Chen H Y 2017 *ACS Nano* **11** 5897
[22] Kamat P V and Hartland G V 2018 *ACS Energy Lett.* **3** 1467
[23] Shi Y, Wang J, Wang C, Zhai T T, Bao W J, Xu J J, Xia X H and Chen H Y 2015 *J. Am. Chem. Soc.* **137** 7365
[24] Liu G, Li P, Zhao G, Wang X, Kong J, Liu H, Zhang H, Chang K, Meng X, Kako T and Ye J 2016 *J. Am. Chem. Soc.* **138** 9128
[25] Wang C, Shi, Y, Yang D R and Xia X H 2018 *Curr. Opin. Electrochem.* **7** 95
[26] Mu X, Hu L, Cheng Y, Fang Y and Sun M 2021 *Nanoscale* **13** 581
[27] Tanaka A, Hashimoto K and Kominami H 2014 *J. Am. Chem. Soc.* **136** 586
[28] Zhao X, Liu C, Yu J, Li Z, Liu L, Li C, Xu S, Li W and Zhang C 2020 *Nanophotonics* **9** 4761
[29] Kong B, Tang J, Selomulya C, Li W, Wei J, Fang Y, Wang Y, Zheng G and Zhao D 2014 *J. Am. Chem. Soc.* **136** 6822
[30] Yin Z, Chen B, Bosman M, Cao X, Chen J, Zheng B and Zhang H 2014 *Small* **10** 3536
[31] Shi Y, Huang J K, Jin L, Hsu Y T, Yu S Y, Li L J and Yang H Y 2013 *Sci. Rep.* **3** 1
[32] Sebastián P, Giannotti M I, Gómez E and Feliu J M 2018 *ACS Appl. Energy Mater.* **1** 1016
[33] Zhou H, Yu F, Liu Y, Sun J, Zhu Z, He R, Bao J, Goddard III W A, Chen S and Ren Z 2017 *Energy Environ. Sci.* **10** 1487
[34] Zhang J, Wang T, Liu P, Liao Z, Liu S, Zhuang X, Chen M, Zschech E and Feng X 2017 *Nat. Commun.* **8** 1
[35] Zhu Y P, Ma T Y, Jaroniec M and Qiao S Z 2017 *Angew. Chem.-Int. Edit.* **56** 1324
[36] Yan K and Lu Y 2016 *Small* **12** 2975
[37] Zhang J, Wang T, Pohl D, Rellinghaus B, Dong R, Liu S, Zhuang X and Feng X 2016 *Angew. Chem.* **128** 6814
[38] Lu J, Xiong T, Zhou W, Yang L, Tang Z and Chen S 2016 *ACS Appl. Mater. Interfaces* **8** 5065
[39] Liu J, Zhang Y H, Bai Z M, Huang Z A and Gao Y K 2019 *Chin. Phys. B* **28** 048101
[40] Tsai C, Abild-Pedersen F and N?rskov J K 2014 *Nano Lett.* **14** 1381
[41] Sun J, Jiang S, Xu J, Li Z, Li C, Yu J, Zhao X, Pan J, Zhang C and Man B 2019 *J. Phys. D: Appl. Phys.* **52** 195402
[42] Gong W, Jiang S, Li Z, Li C, Xu J, Pan J, Huo Y, Man B, Liu A and Zhang C 2019 *Opt. Express* **27** 3483
[43] Chen J, Liu G, Zhu Y Z, *et al.* 2020 *J. Am. Chem. Soc.* **142** 7161
[44] Gao Y, Cheng F, Fang W, Liu X, Wang S, Nie W, Chen R, Ye S, Zhu J, An H, Fan C, Fan F and Fan C 2021 *Natl. Sci. Rev.* **8** 151
[45] Chen Z, Ren W, Gao L, Liu B, Pei S and Cheng H M 2011 *Nat. Mater.* **10** 424
[46] Li C, Xu S, Yu J, Li Z, Li W, Wang J, Liu A, Man B, Yang S and Zhang C 2021 *Nano Energy* **81** 105585
[47] Zhang H X, Li Y, Li M Y, Zhang H and Zhang J 2018 *Nanoscale* **10** 2236
[48] Jaramillo T F, Jørgensen K P, Bonde J, Nielsen J H, Horch S and Chorkendorff I 2007 *Science* **317** 100
[49] Shinagawa T, Garcia-Esparza A T and Takanabe K 2015 *Sci. Rep.* **5** 13801
[50] Ledezma-Yanez I, Wallace W D Z, Sebastián-Pascual P, Climent V, Feliu J M and Koper M T 2017 *Nat. Energy* **2** 1
[51] Li X, Zhu J and Wei B 2016 *Chem. Soc. Rev.* **45** 3145